Science Bulletin 62 (2017) 242–248

Contents lists available at ScienceDirect

Science Bulletin

journal homepage: www.elsevier.com/locate/scib

Article

Reconfigurable single-shot incoherent optical signal processing system for chirped microwave signal compression

Ming Li [a,b,c,*], Shuqian Sun [b,c], Antonio Malacarne [a,d], Sophie LaRochelle [e], Jianping Yao [f], Ninghua Zhu [b,c], Jose Azana [a]

[a] Institut National de la Recherche Scientifique-Énergie, Matériaux et Télécommunications (INRS-EMT), Varennes, Québec J3X 1S2, Canada
[b] State Key Laboratory on Integrated Optoelectronics, Institute of Semiconductors, Chinese Academy of Sciences, Beijing 100083, China
[c] University of Chinese Academy of Sciences, Beijing 100049, China
[d] TeCIP Institute, Scuola Superiore Sant'Anna, Pisa 56124, Italy
[e] Center for Optics, Photonics and Laser (COPL), Université Laval, Québec G1V 0A6, Canada
[f] Microwave Photonics Research Laboratory, University of Ottawa, Ontario K1N 6N5, Canada

ARTICLE INFO

Article history:
Received 19 December 2016
Received in revised form 16 January 2017
Accepted 17 January 2017
Available online 19 January 2017

Keywords:
Fourier optics and signal processing
Analog optical signal processing
Radio frequency photonics
Pulse compression

ABSTRACT

We propose and demonstrate a reconfigurable and single-shot incoherent optical signal processing system for chirped microwave signal compression, using a programmable optical filter and a multi-wavelength laser (MWL). The system is implemented by temporally modulating a specially shaped MWL followed by a suitable linear dispersive medium. A microwave dispersion value up to 1.33 ns/GHz over several GHz bandwidth is achieved based on this approach. Here we demonstrate a single-shot compression for different linearly chirped microwave signals over several GHz bandwidth. In addition, the robustness of the proposed system when input RF signals are largely distorted is also discussed.

1. Introduction

The generation and processing of chirped microwave signals have attracted growing interest for its widely applications, such as modern radar and ultra-fast communications. To break through the speed limitation of the traditional electronic devices, a number of photonic approaches have been proposed for chirped microwave signal generation [1–4]. In addition, received chirped microwave signals need to be compressed for many applications. This is usually realized through matched filtering or correlation using electronic devices. Nowadays, similar optical techniques have been proposed to realize chirped signal compression of broadband chirped microwave signals. For instance, Weiner's group [5–7] demonstrated a chirped signal compression system by achieving the desired microwave phase filtering through an optical filtering. However, this scheme requires a linear optical filter with outstanding resolution (about sub-GHz range), increasing the system cost and complexity of the chirped pulse compressor. Additionally, Yao's group [8] demonstrated a chirped microwave compression system using a microwave photonics filter. As a main disadvantage, this compression system is inflexible, since the structure of a fabricated FBG cannot be adjusted. That means the proposed system can be only used for optimal operation with a specific, predefined chirped signals.

Incoherent photonic generation and processing of microwave signals avoid cumbersome and costly pulsed lasers by using an incoherent broadband light source. This methodology has attracted great interest for a wide range of important applications, such as implementation of microwave photonics filter [9–14], arbitrary waveform generation [15–18] and Fourier transformation [19]. The main limitation of a conventional incoherent photonic signal processing technique is the extremely low signal-to-noise ratio (SNR) of the output signal [15–16]. The low SNR is a result of the spontaneous emission of a purely incoherent light source such as amplified spontaneous emission (ASE). Therefore, signal manipulation and measurement cannot be achieved in a single shot using a conventional incoherent-light (referred just as "incoherent" in the rest of the paper) microwave signal processing system [15]. Thousands of times average is typically required to mitigate the white noise that is intrinsically present at the output of an incoherent microwave signal processing system, restricting application of the system to processing periodically repeating signals. Some

* Corresponding author.
E-mail addresses: ml@semi.ac.cn (M. Li), azana@emt.inrs.ca (J. Azana).

http://dx.doi.org/10.1016/j.scib.2017.01.021

schemes have been proposed to overcome this problem. For instance, a spectrum-sliced microwave photonic filter has been proposed to mitigate the noise in the signal processing band [20]. However, the relative broad linewidth of the comb-like optical filter increases the low-frequency bandwidth-limitation of the microwave photonic filter.

In this paper, we report a reconfigurable and single-shot incoherent optical signal processing system for chirped microwave signal compression. To be noted that the problem of chirped microwave signal compression is a relevant example of processing functionality where one cannot afford operation over multiple shots. In most practical cases, a single, isolated copy of the chirped microwave signal will need to be processed. In our proposed scheme, we use a multi-wavelength laser (MWL) as the incoherent light source, rather than a continuous spectrum. Notice that a scheme based on a similar MWL design has been previously employed in Ref. [21] to implement a single-shot photonic time-intensity integrator. Due to the use of the MWL, the SNR of the output signal gets improved significantly such that operation in a single-shot is possible. Moreover, our design enables realization of a fiber-based microwave dispersive line with an extremely large chromatic dispersion (i.e., a few ns^2, equivalent to several thousand kilometers of conventional single-mode fiber) [22–24]. Such an accomplishment is achieved using a design called time-spectrum convolution (TSC) system [25]. The effective dispersion of microwave signal through this TSC system is orders of magnitude higher than the actual physical optical dispersion used in the system. Furthermore, the induced dispersion on the microwave signal is tunable by adjusting the programmable optical filter or by changing the optical dispersive medium [26], such that the proposed scheme is fully reconfigurable. Different chirped microwave signals with GHz-bandwidth are successfully compressed and the robustness of the proposed system when input RF signals are largely distorted is also discussed.

2. Principle

Fig. 1 shows the scheme of our proposed compression system. An all-fiber MWL with channel spacing of 100 GHz is employed. The total bandwidth of the MWL is about 4 THz, with the linewidth of each channel narrower than 100 kHz [27]. A programmable optical filter (Finisar WaveShaper 4000S) is then used to shape the spectrum of the MWL. The resolution of the optical filter is about 10 GHz and its total filter range is 5 THz. The filtered broadband MWL is then launched into a 20-GHz intensity Mach-Zehnder modulator (MZM) for modulation. The input signal of the MZM is a chirped RF signal generated from an arbitrary waveform generator (AWG, AWG7122C, Tektronix Inc.). Then the modulated optical signal is sent to a single mode fiber (SMF) and detected by a 25-GHz photo-detector (PD). As mentioned, the bandwidth of the PD (25 GHz) is much narrower than the channel spacing of the MWL (100 GHz), so the beating signal between different frequency lines cannot be detected by the PD. Thus the intensity noise induced by beating will not be involved in the output waveform. In addition, since the linewidth of each laser is much lower than the modulation frequency, the modulation noise could be ignored.

As shown in Fig. 1, the input electric field $E_{0,\omega}(t)$ before the MZM is given by

$$E_{0,\omega}(t) = \sqrt{S(\omega)}Comb(\omega)\mathrm{e}^{\mathrm{i}[\omega t+\phi(\omega)]}, \tag{1}$$

where $S(\omega)$ is the intensity envelope of the MWL spectrum, $\phi(\omega)$ denotes the phase noise of each frequency. The spectrum of the MWL can be approximately expressed as

$$Comb(\omega) \propto \sum_{n=-\infty}^{\infty} \delta(\omega - n\Delta\omega), \tag{2}$$

where n is the order of channels, $\Delta\omega$ is the free spectral range (FSR) of the MWL. The electric field $E_{1,\omega}(t)$ after the MZM can be obtained as

$$E_{1,\omega}(t) = \sqrt{S(\omega)}Comb(\omega)x(t)\mathrm{e}^{\mathrm{i}[\omega t+\phi(\omega)]}, \tag{3}$$

where $x(t)$ represents the input microwave signal. After propagating in the SMF with dispersion value $\ddot{\Phi}$, the electric field will becoming the following form [15]:

$$E_{2,\omega}(t) = \sqrt{S(\omega)}Comb(\omega)x_c(t - \ddot{\Phi}\omega)\mathrm{e}^{\mathrm{i}[\omega t+\phi(\omega)]}, \tag{4}$$

in which x_c is the modulation signal after dispersion. When the bandwidth of the microwave signal $\Delta\omega_x$ is small enough so that the input pulse is not affected by the dispersion in SMF, we have $x_c(t) \approx x(t)$; this can be approximately estimated by the inequality: $\Delta\omega_x^2\ddot{\Phi} \ll 8\pi$. Then the output field can be written as

$$\begin{aligned} E_2(t) &= \int_{-\infty}^{\infty} \sqrt{S(\omega)}Comb(\omega)x(t - \ddot{\Phi}\omega)\mathrm{e}^{\mathrm{i}[\omega t+\phi(\omega)]}\mathrm{d}\omega \\ &= \sum_{n=-\infty}^{\infty} \sqrt{S(n\Delta\omega)}x(t - n\ddot{\Phi}\Delta\omega)\mathrm{e}^{\mathrm{i}(n\Delta\omega t+\phi_n)}, \end{aligned} \tag{5}$$

in which $\phi(\omega)$ is replaced by ϕ_n. Since the linewidth of each channel of the MWL is around tens of kHz [27], much narrower than the modulation frequency, the modulation-induced noise could be mitigated significantly [20]. Therefore, no average is required for chirped microwave signal compression. To be more accurate, the detecting process inside the PD can be expressed as following equation [28]

$$\begin{aligned} I_2(t) &\propto \frac{1}{T_m}\int_{t-T_m/2}^{t+T_m/2} E_2(t')E_2^*(t')\mathrm{d}t' \\ &= \frac{1}{T_m}\int_{t-T_m/2}^{t+T_m/2} \sum_{n=-\infty}^{\infty}\sum_{m=-\infty}^{\infty} \sqrt{S(n\Delta\omega)S(m\Delta\omega)}x(t' \\ &\quad - n\ddot{\Phi}\Delta\omega)x^*(t' - m\ddot{\Phi}\Delta\omega)\mathrm{e}^{\mathrm{i}(n-m)\Delta\omega t'}\mathrm{e}^{\mathrm{i}(\phi_n-\phi_m)}\mathrm{d}t', \end{aligned} \tag{6}$$

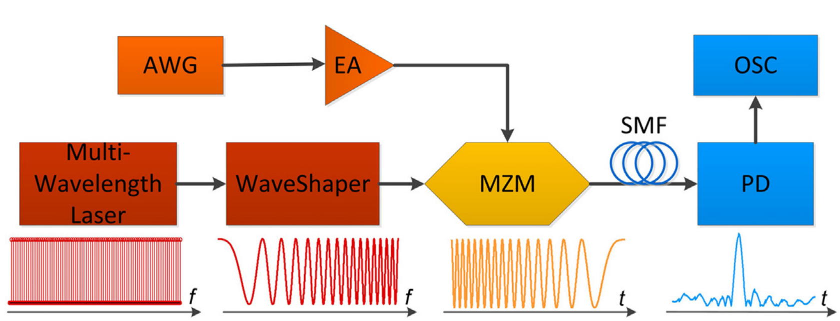

Fig. 1. The experimental setup of our proposed microwave signal compression system. AWG: arbitrary waveform generator; OSC: real time oscilloscope; EA: electric amplifier; MZM: Mach-Zehnder modulator; SMF: single mode fiber; PD: photodetector;

where T_m is the response time of the PD. The bandwidth of the PD can be expressed as $1/T_m$. The beating signal will not be detected if the FSR of the MWL is larger than the PD bandwidth. Thus, the integral is valid only for $n = m$. Thus the output current of the PD can be rewritten as

$$I_2(t) \propto \sum_{n=-\infty}^{\infty} S(n\Delta\omega)X(t - n\ddot{\Phi}\Delta\omega) \propto \int_{-\infty}^{\infty} S(\omega)X(t - \ddot{\Phi}\omega)\mathrm{d}\omega$$
$$= \frac{1}{\ddot{\Phi}} S(\frac{t}{\ddot{\Phi}}) \otimes X(t), \tag{7}$$

where $X = |x|^2$, and $\otimes$ denotes convolution. From Eq. (7) we can see that the output signal intensity is the convolution between the time-mapped spectrum of MWL and the intensity of input signal. Meanwhile, the noise induced by beating interference is also avoided.

As shown in Fig. 1, the MWL spectrum is filtered by a WaveShaper with a quadratic phase variation. The envelope of the filter spectrum can be expressed by

$$S(\omega) \propto C_1 \Re[\exp(\mathrm{i}a_{s1}\omega + \mathrm{i}\frac{a_{s2}}{2}\omega^2)], \tag{8}$$

where C_1 is the profile of the chirped envelope of the spectrum, $\Re$ represents the real part, a_{s1} and a_{s2} denote the weights of the linear and quadratic phase terms, respectively. The time-domain version of $S(\omega)$can be written as

$$S(\frac{t}{\ddot{\Phi}}) \propto C_1 \Re[\exp(\mathrm{i}\omega_0 t + \mathrm{i}\frac{t^2}{2\ddot{\Phi}'})], \tag{9}$$

in which $\omega_0 = a_{s1}/\ddot{\Phi}$ denotes the effective central angular frequency and $\ddot{\Phi}' = \ddot{\Phi}^2/a_{s2} = N\ddot{\Phi}$ ($N = \ddot{\Phi}/a_{s2}$) represents the dispersive value for microwave signal induced by the TSC system. Since a_{s2} can be quite smaller than $\ddot{\Phi}$, the multiplication factor N can be made much larger than 1 and an ultrahigh dispersion $\ddot{\Phi}'$ is then achieved. It is worth noting that the operation bandwidth of the TSC system, $\Delta\omega$, is limited by the bandwidth of MWL, $\Delta\omega_{\mathrm{opt}}$, which can be expressed as $\Delta\omega = \Delta\omega_{\mathrm{opt}}/N$ [19].

The intensity of a linearly chirped microwave signal can be expressed as

$$X(t) \propto C_2 \Re[\exp(\mathrm{i}a_{X1}t + \mathrm{i}\frac{a_{X2}}{2}t^2)], \tag{10}$$

where C_2 denotes the profile of the chirped microwave signal, a_{X1} and a_{X2} represent the weights of the linear and quadratic phase terms respectively. Then the profile of the output intensity is given by

$$|I_2(t)| \propto |\int C_1C_2 \exp(\mathrm{i}\omega_0\tau + \mathrm{i}\frac{\tau^2}{2\ddot{\Phi}'}) \times X(t-\tau)\mathrm{d}\tau|$$
$$= |\int C_1C_2 \exp[\mathrm{i}(\omega_0 - a_{X1})\tau - \mathrm{i}a_{X2}t\tau + \mathrm{i}(\frac{1}{\ddot{\Phi}'} + a_{X2})$$
$$\times \frac{\tau^2}{2}]\mathrm{d}\tau|. \tag{11}$$

If a_{X1} and a_{X2} satisfy the condition of

$$a_{X1} = \omega_0 \text{ and } a_{X2}\ddot{\Phi}' = -1, \tag{12}$$

the maximum compression will be achieved. Eq. (11) can then be rewritten as

$$|I_2(t)| \propto \{\Im[C_1C_2]\}_{\omega = a_{X2}t}, \tag{13}$$

where $\Im$ represents Fourier transform. Since the profiles of the chirped envelope of the MWL spectrum and the input microwave signal are rectangular, the output intensity has a sinc-like envelope. It can be seen from Eqs. (11)–(13), the chirped waveform can be largely compressed by suitably programming the optical filter, which means our proposed system is fully reconfigurable. It is worth noting that no averaging is required for the output signal measurement when two conditions are satisfied: the modulation frequency is larger than the linewidth of the MWL; and the PD's bandwidth is narrower than the wavelength spacing. More details about noise analysis can be found in Ref. [20].

3. Experimental results

The MWL is spectrally shaped to exhibit a linearly chirped sinusoidal envelope to achieve the desired dispersion effect on the modulating microwave signal following optical dispersion through optical fiber. The spectrum of the shaped MWL is shown in Fig. 2a. In our first experiment, a 2.5-km-long SMF is employed as the dispersive element. The corresponding time-bandwidth relation of the dispersive line is shown in Fig. 2b (red dash lines). An effective dispersion approaching 0.23 ns/GHz (equal to the dispersion provided by a 1711-km-long SMF) with a bandwidth between 2.5 and 8.4 GHz is achieved. Based on the specifications of the fiber dispersive line, this is used for compression of an input chirped microwave signal covering the whole signal processing bandwidth. The microwave signal is generated using an AWG. As can be seen in Fig. 3a, the input RF signal $x(t)$ is linearly chirped from 1.25 to 4.20 GHz. Since the input of the processing system is actually $X = |x|^2$, the effective frequency of the linearly chirped microwave signal is from 2.5 to 8.40 GHz. The output signal is monitored by a real-time oscilloscope (DPO70804, Tektronix Inc.), as shown in Fig. 3b. The bandwidth of our real-time oscilloscope is 8 GHz, with a sampling rate of 25 Gs/s. No averaging has been used in these measurements. The pulse duration of the compressed signal is about 0.1 ns, 15 times narrower than the original input signal (1.5 ns).

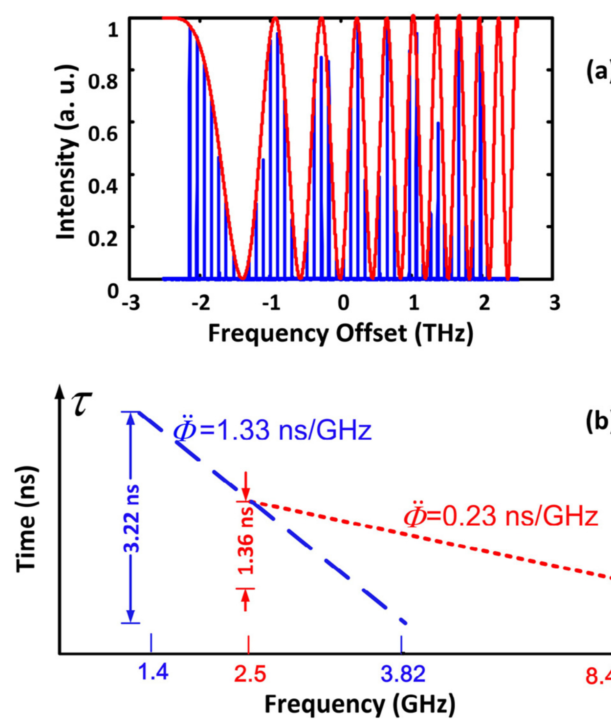

Fig. 2. Shaped MWL spectrum and time-bandwidth relation of the dispersive line. (a) Measured spectrum of a shaped MWL, (b) the time-bandwidth relation of the dispersive line based on the shaped MWL in (a) and different dispersive elements (i.e., 2.5 km (red) and 6 km (blue) SMF).

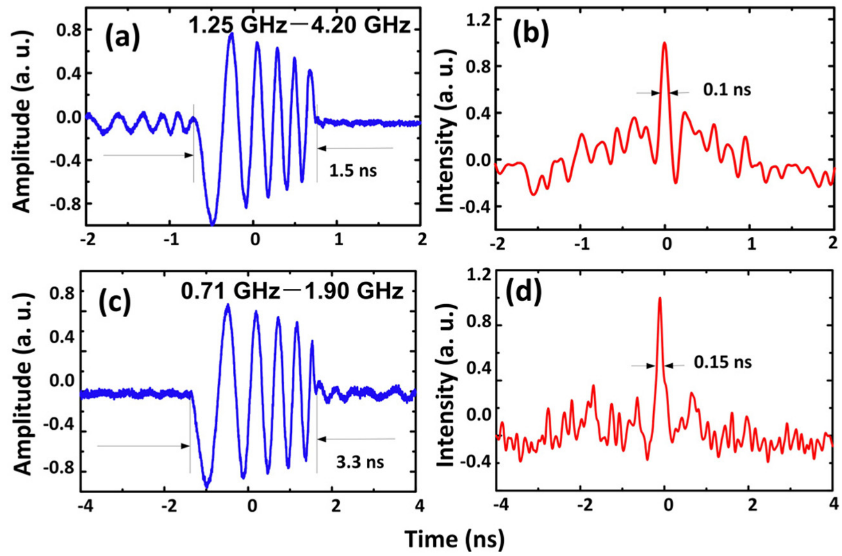

Fig. 3. Reconfigurability via tuning dispersion. (a) Input linear chirped RF signal with frequency from 1.25 to 4.20 GHz and the corresponding output signal (b) using a 2.5-km-long SMF. (c) Input linear chipred RF signal with frequency ranging from 0.71 to 1.90 GHz and the corresponding output signal (d) using a 6-km-long SMF. The temporal waveforms of output signals are measured using a real-time oscilloscope without averaging.

3.1. Reconfigurability via tuning dispersion

By changing a new SMF with different length (6 km), the chirped microwave compression system can be easily adjusted. As shown in Fig. 2b, the effective dispersion value for microwave signal is tuned from 0.23 to 1.33 ns/GHz (equal to the dispersion provided by a 9896 km SMF) with a bandwidth ranging from 1.4 to 3.82 GHz. As observed in Fig. 3c, an input RF signal with a bandwidth of 1.19 GHz (frequency from 0.71 to 1.9 GHz) and pulse width of 3.3 ns is launched into the MZM. The output signal is measured by our real-time oscilloscope with no averaging (Fig. 3d). Again, the chirped input signal is successfully compressed from 3.3 to 0.15 ns, with a compression factor of 22.

3.2. Reconfigurability via shaping spectrum of the MWL

The compression system can also be reconfigured by programming the optical filter. To demonstrate the flexibility of our proposed scheme, the spectral envelope of the MWL is changed to be 1/2 chirp rate of the spectrum shown in Fig. 2a. When the length of the employed SMF is 2.5 km, an effective dispersion value of 0.46 ns/GHz (equal to the dispersion value provided by a 3423-km-long SMF) is achieved, with an operating bandwidth between 2.88 and 5.88 GHz (Fig. 4b). Here a chirped signal with 1.9 GHz bandwidth (from 1.0 to 2.9 GHz) and 1.25 ns time duration is launched into the MZM, as shown in Fig. 4c. After processing by the TSC system, the chirped microwave signal is compressed from 1.25 ns to about 0.1 ns with a compression factor of 12.5 (measured without averaging, see Fig. 4d). From this experiment we can conclude that the proposed microwave signal compression scheme shows high flexibility for processing various chirped microwave signals by programming the spectrum of the optical filter.

3.3. Robustness of the chirped microwave signal compression system

In order to test the robustness of our proposed microwave compression system, white noise is introduced to the input microwave signal shown in Fig. 3c. Because of the presence of white noise, the

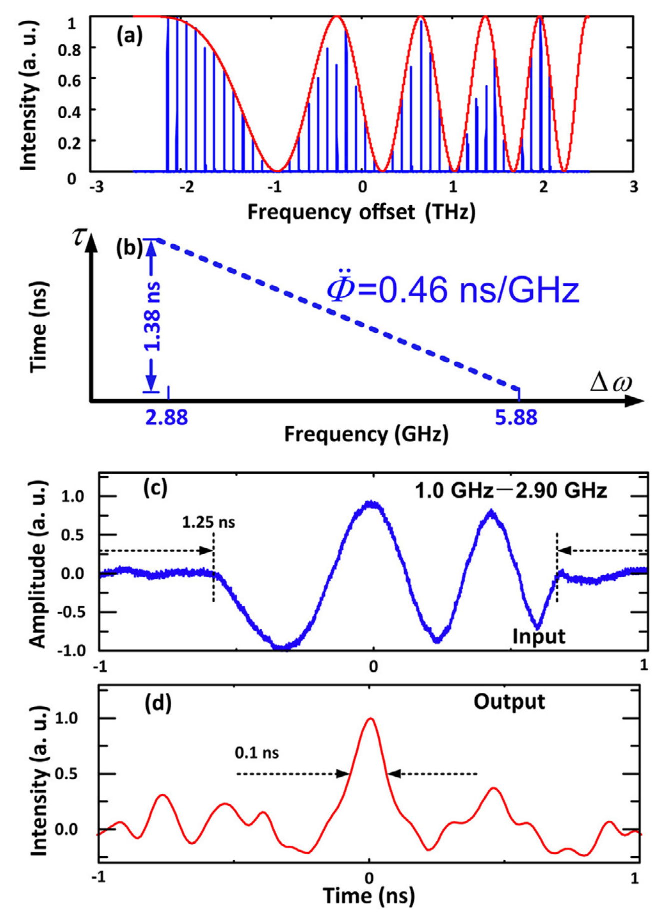

Fig. 4. Reconfigurability via shaping spectrum of the MWL. (a) Measured spectrum of the MWL after a optical filter, with a 1/2 chirp rate of the spectral envelope shown in Fig. 2a. (b) The time-bandwidth relation of the reconfigured compression system. (c) Linearly chirped input signal and the corresponding compressed signal (d). The waveforms shown in (c) and (d) are measured using a real-time scope without averaging.

time duration of the signal seems to be expanded slightly (to about 3.8 ns). And the SNR of the RF signal is as low as 0 dB, as observed in Fig. 5a. Here the spectrum envelope of the MWL is the same as the spectrum shown in Fig. 2a. After propagating through a 6-km-long SMF, the input waveform is compressed by 35 times (the pulse width of the output signal is about 0.11 ns) as shown in Fig. 5b. The measurement result of Fig. 5b is obtained by a real-time oscilloscope without any averaging. As shown, the compressed pulse can be recognized obviously. Results will be quite different if the MWL is replaced by a superluminescent diode (SLD), which is a continuous broadband light source. Using the same input signal, the output waveform of the system without any average is too noisy to be recognized (Fig. 5c). Even though a 50 times average is employed using a sampling oscilloscope (CSA8000, Tektronix Inc.), the compressed pulse (Fig. 5d) still has poor SNR and smaller compression ratio compared with the result shown in Fig. 5b. From the comparison we can conclude that our proposed system using MWL as the incoherent source can achieve a single shot compression with high SNR, even though the input RF signal is largely distorted.

4. Discussion

In order to obtain a high-quality compressed signal, the condition described by Eq. (12) need to be satisfied. Besides the chirp parameters of filtered spectra and input signals, spectral region and resolution of optical sources can also affect the output quality. In the following discussions, we will see how the system performance is influenced by spectral range and resolution of the MWL.

4.1. The spectral range of MWL

To analyze the influence of spectral range of MWL on the system, the compression performance with different spectral ranges are simulated. The spectra of MWL employed in this simulation are shown in Fig. 6a–c. As shown, the spectral range of these spectra varying from 4 to 8 THz. Except for the spectral range, channel

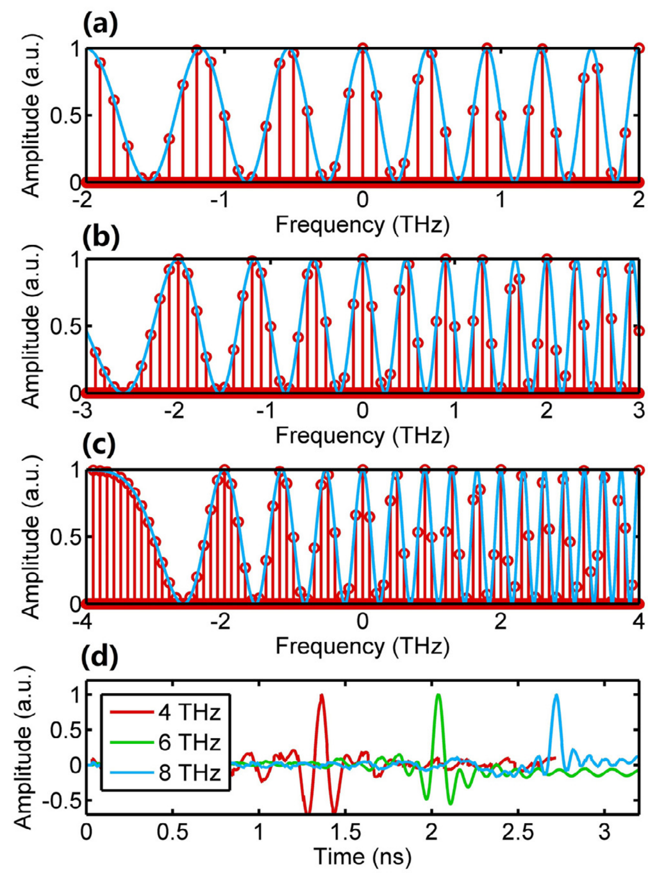

Fig. 6. System performance using different spectral range of MWL. (a)–(c) Spectra of filtered MWL with spectral range of 4, 6 and 8 THz. Red lines represent the spectra of MWL, while blue lines denote the spectral envelope of optical filter. The channel spacing is 100 GHz in all the three cases and the chirp rate is also unchanged ($a_{s1} = 2 \times 10^{-12}$ s, $a_{s2} = 8 \times 10^{-26}$ s^2/rad). (d) The corresponding output waveforms shown in different colors.

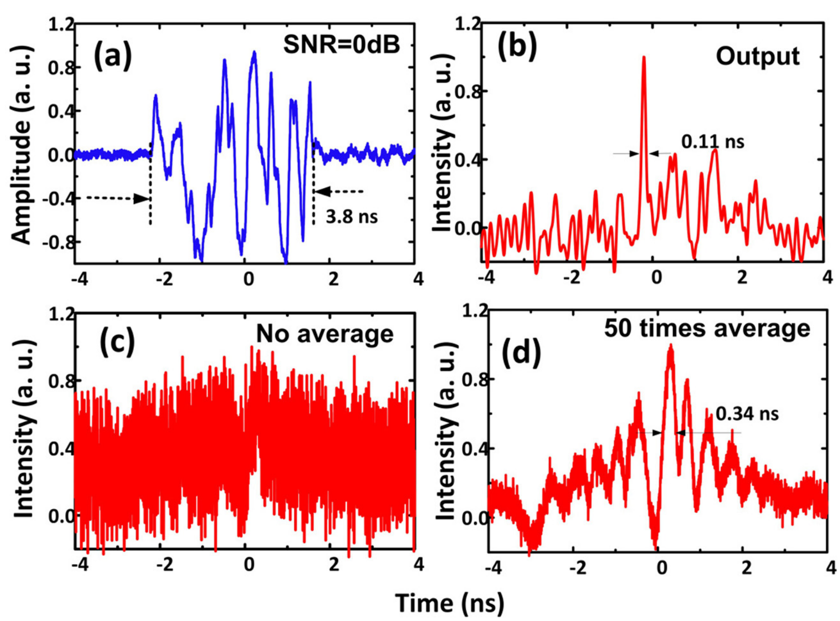

Fig. 5. Robustness of the chirped microwave signal compression system. (a) Chirped input RF signal shown in Fig. 3c with white Gaussian noise, in which the SNR is as low as 0 dB. (b)The compressed signal using an MWL as the incoherent source. (c) When a SLD is used as the incoherent light source, the measured compressed signal without average is difficult to recognized. (d) Even though a 50 times average is employed, the output signal still has a low SNR and the compression ratio is smaller than (b).

spacing (100 GHz) and chirp parameters ($a_{s1} = 2 \times 10^{-12}$ s, $a_{s2} = 8 \times 10^{-26}$ s^2/rad) of the MWL spectra remain unchanged. The optical dispersion is set to be $\ddot{\Phi} = 5.41 \times 10^{-23}$s^2/rad, equal to the dispersion induced by a 2.5-km-long SMF. Based on the condition described by Eq. (12), chirp parameters of the input signal is determined, i.e. $a_{X1} = 3.7 \times 10^{10}$ rad/s and $a_{X2} = 2.7 \times 10^{19}$ rad/s^2.

The output signals under different spectral ranges are shown in Fig. 6d using different colors. It can be seen obviously that the sideband of output waveforms are suppressed with the increase of spectral range. That means a broader spectrum is required for a high-quality output waveform.

4.2. The channel spacing of MWL

Apart from spectral range of the optical sources, spectral resolution is also an important factor related to the quality of output signals. Fig. 7a–c shows the simulated spectra of MWL with different channel spacing (200, 100 and 50 GHz respectively). Other spectral parameters, such as spectral range (4 THz) and chirp rate ($a_{s1} = 2 \times 10^{-12}$ s, $a_{s2} = 8 \times 10^{-26}$ s^2/rad) remain unchanged in the simulation. Again, the input chirped RF signal is chosen according to Eq. (12). The corresponding output signals using three spectral resolutions are shown in Fig. 7d. Compared to the output signals with spectral channel spacing of 100 GHz (in green) and 50 GHz (in blue), the output waveform with 200 GHz spectral resolution has much more sidebands and variations. Obviously, the poor quality results from the large channel spacing of MWL. As shown in Fig. 7a, the spectrum is too sparse to recover the spectral envelope of optical filter. System performance will be much better if the channel spacing is reduced twice. As shown in Fig. 7d, the sideband of the green line is largely suppressed compared to the waveform shown in red. And the spectral outline of the optical filter can be described basically by the spectrum of MWL (Fig. 7b). However, when the channel spacing is further reduced, e.g. to 50 GHz, there is hardly any improvement of the output signal (see the blue line in Fig. 7d), even though the filter outline is well described by the spectrum of MWL (Fig. 7c). That means a spectrum with very high resolution is not necessary for a good system performance. It is not difficult to accept this conclusion if we are familiar with Nyquist sampling theorem.

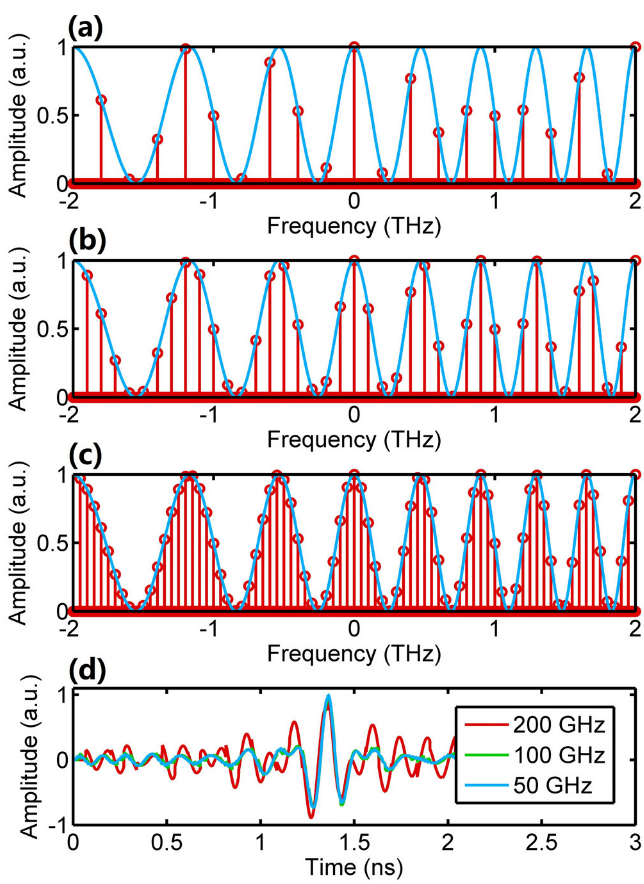

Fig. 7. System performance using different spectral resolutions. (a)-(c) Spectra of filtered MWL with channel spacing of 200, 100 and 50 GHz. Red lines represent the spectra of MWL while blue lines denote the spectral envelope of optical filter. The spectral range is 4 THz in all the three cases and the chirp rate is also unchanged ($a_{s1} = 2 \times 10^{-12}$ s, $a_{s2} = 8 \times 10^{-26}$ s^2/rad). (d) The corresponding output waveforms shown in different colors.

5. Conclusion

In conclusion, a reconfigurable and single-shot incoherent-light signal processing system for chirped microwave signal compression is proposed and realized. Thanks to the use of a MWL, the SNR of the system is improved significantly. By tuning the programmable optical filter or by changing the dispersion of the dispersive medium, the system can be fully reconfigurable to adapt to the specifications (e.g., frequency chirp) of the incoming input signals. Different chirped pulses with GHz bandwidth have been optimally compressed by several tens times. The compression system shows outstanding robustness in a single-shot performance even though the SNR of input signals is strongly deteriorated.

Conflict of interest

The authors declare that they have no conflict of interest.

Acknowledgments

This work was supported by research grants from NSERC (Canada) agencies, and also partly supported by the National Natural Science Foundation of China (61522509, 61377002 and 61090391), Beijing Natural Science Foundation (4152052) and the National High-Tech Research and Development Program of China (2015AA017102). M. L. was supported partly by the Thousand Young Talent Program.

References

[1] Rihaczek AW. Principles of high-resolution Rada. Norwood, MA: Artech House; 1996.
[2] Li M, Yao JP. Photonic generation of continuously tunable chirped microwave waveforms based on a temporal interferometer incorporating an optically-pumped linearly-chirped fiber Bragg grating. IEEE Trans Microw Theory Tech 2011;59:3531–7.
[3] Khan MH, Shen H, Xuan Y, et al. Ultrabroad-bandwidth arbitrary radiofrequency waveform generation with a silicon photonic chip-based spectral shaper. Nat Photon 2010;4:117–22.
[4] Shi JW, Kuo FM, Chen NW, et al. Photonic generation and wireless transmission of linearly/nonlinearly continuously tunable chirped millimeter-wave waveforms with high time-bandwidth product at W-band. IEEE Photon J 2012;4:215–23.
[5] Hamidi E, Weiner AM. Phase-only matched filtering ultrawideband arbitrary microwave waveforms via optical pulse shaping. J Lightwave Technol 2008;26:2355–63.
[6] Hamidi E, Weiner AM. Post-compensation of ultra-wideband antenna dispersion using microwave photonic phase filters and its applications to UWB systems. IEEE Trans Microw Theory Tech 2009;57:890–8.
[7] Weiner AM. Ultrafast optical pulse shaping: a tutorial review. Opt Commun 2011;284:3669–92.
[8] Wang C, Yao JP. Chirped microwave pulse compression using a photonic microwave filter with a nonlinear phase response. IEEE Trans Microw Theory Techn 2009;57:496–504.
[9] Capmany J, Novak D. Microwave photonics combines two worlds. Nat Photon 2007;1:319–30.
[10] Minasian RA. Photonic signal processing of microwave signals. IEEE Trans Microw Theory Techn 2006;54:832–46.

[11] Seeds AJ, Williams KJ. Microwave photonics. J Lightwave Technol 2006;24:4628–41.
[12] Yao JP. Microwave photonics. J Lightwave Technol 2009;27:314–35.
[13] Capmany J, Ortega B, Pastor D, et al. Discrete-time optical processing of microwave signals. J Lightwave Technol 2005;23:702–23.
[14] Zou XH, Pan W, Yan LS. All-optical processing to optical and radio frequency (RF) signals. Sci Bull 2015;60:2151–3.
[15] Dorrer C. Statistical analysis of incoherent pulse shaping. Opt Express 2009;17:3341–52.
[16] Torres V, Lancis J, Andres P, et al. Reconfigurable RF-waveform generation based on incoherent-filter design. J Lightwave Technol 2008;26:2476–83.
[17] Bolea M, Mora J, Ortega B, et al. Optical arbitrary waveform generator using incoherent microwave photonic filtering. IEEE Photon Technol Lett 2011;23:618–20.
[18] Bolea M, Mora J, Ortega B, et al. Nonlinear dispersion-based incoherent photonic processing for microwave pulse generation with full reconfigurability. Opt Express 2012;20:6728–36.
[19] Park Y, Azaña J. Ultrahigh dispersion of broadband microwave signals by incoherent photonic processing. Opt Express 2010;18:14752–61.
[20] Yi X, Minasian RA. Noise mitigation in spectrum sliced microwave photonic signal processors. J. Lightwave Technol 2006;24:4959–65.
[21] Malacarne A, Ashrafi R, Li M, et al. Single-shot photonic time-intensity integration based on a time-spectrum convolution system. Opt Lett 2012;37:1355–7.
[22] Li M, Azana J. Programmable and single-shot chirped microwave pulse compression using an optical fiber-based microwave dispersive line. Information Science, Signal Processing and their Applications (ISSPA), 2012 11th International Conference on. IEEE; 2012, p.1396–1400.
[23] Li M, Malacarne A, LaRochelle S et al. Reconfigurable and single-shot chirped microwave pulse compression using a time-spectrum convolution system. Microwave Photonics, 2011 International Topical Meeting on & Microwave Photonics Conference, 2011 Asia-Pacific, MWP/APMP. IEEE; 2011, p, 9–12.
[24] Li M, Malacarne A, Belhadj N, et al. Reconfigurable optical fiber-based microwave dispersive line for single-shot chirped microwave pulse compression. Optical Fiber Communication Conference. Optical Society of America, OW4H.; 2012, p.1
[25] Park Y, Azaña J. Optical signal processors based on a time-spectrum convolution. Opt Lett 2010;35:796–8.
[26] Kim J, Bae J, Han YG, et al. Effectively tunable dispersion compensation based on chirped fiber Bragg grating without central wavelength shift. IEEE Photon Technol Lett 2004;16:849–51.
[27] Kim Y, Doucet S, LaRochelle S. 50-channel 100-GHz-spaced multiwavelength fiber lasers with single-frequency and single-polarization operation. IEEE Photon Technol Lett 2008;20:1718–20.
[28] Lauterborn W, Kurz T. Coherent optics: fundamentals and applications. 2nd ed. Springer; 2003.